*35th EPS Conference on Plasma Phys. Hersonissos, 9 - 13 June 2008 ECA Vol.**32D**, P-2.024 (2008)*

The role of the H-mode pedestal on global confinement in hybrid scenarios in DIII-D and ASDEX Upgrade

C.F. Maggi[1], R.J. Groebner[2], C. Angioni[1], J. Candy[2], C. Konz[1], A.W. Leonard[2], T. Hein[1], L.D. Horton[1], C.C Petty[2], A.C.C. Sips[1], R.E.Waltz[2], ASDEX Upgrade[1] and DIII-D[2] Teams

[1]MPI für Plasmaphysik, EURATOM Association, D-85748 Garching, Germany
[2]General Atomics, San Diego, California 92186, USA

1. Power scans in ASDEX Upgrade and DIII-D hybrid discharges - Hybrid discharges (improved H-modes in ASDEX Upgrade, AUG) are characterized by confinement factors H98(y,2) > 1 and total beta $2 < \beta_N < 3.5$. Dedicated power (total beta) scans have been performed in AUG and DIII-D with the aim of i) studying the role of the H-mode pedestal on global confinement in hybrid discharges, ii) comparing pedestals in AUG and DIII-D and iii) investigating the variation of the pedestal structure with beta and plasma shape.

The AUG power scans were carried out at $I_P = 1.0$ MA, $B_T = 2.4$ T (2005 campaign [1]) and 2.55 T (2008 campaign with an all W wall [2]) and average triangularity $\delta = 0.2 – 0.3$. The DIII-D power scans were performed at similar $q_{95} \sim 4.6$ ($I_P \sim 1.1$ MA and B_T varied from -1.9 to -2.14 T), fixed density $n_e \sim 4 \times 10^{19}$ m^{-3} and at two different plasma shapes, so as to differentiate between power and shape dependence of the pedestal pressure. The two low single null plasma shapes are a high $\delta = 0.5$ shape optimized for hybrid studies in DIII-D and the low δ AUG shape ($\delta = 0.23$) matched in DIII-D. In the high δ shape, a power scan at fixed low toroidal rotation – achieved using balanced beam injection [3] - was also performed.

Hybrid operation was obtained in the matched AUG shape in DIII-D using the AUG improved H-mode recipes, with and without additional heating during the plasma current ramp-up phase (early and late heating schemes). In the stationary phase, the discharges with early and late heating were very similar both in terms of global and pedestal plasma parameters. The MHD behaviour was also similar in the two cases and similar to that observed in the hybrid discharges at high δ. 3/2 NTMs and 1/1 activity, sawtoothing at lower β_N values and almost continuous at higher β_N, was observed. These findings are in qualitative agreement with observations in AUG, where the late heating scheme even results in a better discharge performance compared to the early heating scheme at moderate β_N values [4].

2. Global and pedestal confinement - The H98(y,2) confinement factor increases with total β_N both in the DIII-D and AUG power scans, but is higher in the $\delta = 0.5$ shape at a given β_N in DIII-D. In the DIII-D power scans, at low β_N the discharge with late heating has a higher H98(y,2) factor than the early heating counterpart, despite very similar input parameters. In this case, the different core MHD, namely 4/3 NTMs replaced later on in the discharge by fishbones and sawtooth activity, is correlated with higher confinement, in analogy with findings in AUG [4].

However, a different variation of the pedestal beta, β_N^{PED}, with total thermal beta is found in the two plasma shapes in DIII-D (Fig. 1): β_N^{PED} increases with $\beta_{N,th}$ at low δ, although more weakly than observed in AUG, but saturates with beta at high δ, in contrast to what observed in a dedicated power scan subsequently performed at DIII-D [5]. In DIII-D with high δ shape the core stored energy increases with power at constant pedestal energy, hence the confinement enhancement is due to core physics. In AUG, β_N^{PED} increases linearly with $\beta_{N,th}$ as reported previously [1].

3. Scaling of the pedestal width - A scaling for the pedestal width Δ has been proposed, based on the DIII-D pedestal database, where $\Delta \sim \beta_{pol,PED}^{1/2}$ [5] and $\beta_{pol,PED}$ is the poloidal beta calculated at the pedestal. Using this empirical scaling for the pedestal width as input and assuming the pressure gradient in the pedestal as given by the Peeling-Ballooning model, the pedestal top pressure measured in a series of DIII-D experiments can be predicted within the experimental accuracy [5]. Recent dimensionless parameter studies of the pedestal width in JT-60U indicate no (or weak) ρ^* dependence and a $\beta_{pol,PED}$½ dependence of the pedestal width [6].

We want to test the scaling of the pedestal width in AUG and on the DIII-D dataset of this study. All T_e, n_e and T_i profiles within the long (> 3 x τ_E) stationary time window selected for the analysis are combined together according to a chosen fraction of time before the ELM crash and then fit with hyperbolic tangent functions to derive the pedestal widths. One issue is what is the relevant pedestal width, since previous analysis has shown that the widths of the individual parameters do differ also systematically as the power/beta is increased [1]. The approach adopted in [5] is to define the pedestal width as the average of Δ_{Te} and Δ_{ne}, whereas in [6] the scaling is obtained from Δ_{Ti}. In line with previous studies, we investigate here the scaling of the pedestal width of each parameter separately. We find that given the variation in $\beta_{pol,PED}$ in the experiments, the width scaling is consistent with a $\Delta \sim \beta_{pol,PED}^{1/2}$ dependence, but also a linear dependence of the pedestal width with $\beta_{pol,PED}$ cannot be excluded (Fig. 2). This result applies to the pedestal widths of T_e, T_i and n_e of the DIII-D data and to the T_e widths of the AUG powers scans in [1]. The large scatter in the T_e and T_i pedestal widths from the 2008 AUG experiments unfortunately prevents us from drawing any conclusion from these data. In AUG the n_e pedestal width doesn't show any dependence on β_{PED}, as found in previous studies.

4. Edge stability analysis - An additional goal of this study is to confront the model-based analysis of [5] with the measured pedestal top values from the AUG and DIII-D power scans of this study. To this aim, work has started on edge stability analysis of the beta scans reported here using the linear MHD stability code ILSA [7]. Fig. 3 compares the theoretical growth rates for peeling-ballooning edge modes as a function of toroidal mode number for two AUG equilibria and two DIII-D equilibria. For the AUG case at β_N = 2.7 (Fig. 3, #20116, red trace) we find a more pronounced ballooning component of the edge mode compared to the DIII-D discharge at low δ (AUG shape) and β_N = 2.5 (Fig.3, green trace). The DIII-D equilibrium at δ = 0.5 and β_N = 2.7 exhibits a more pronounced peeling

character of the edge instability, as shown by the peaking of the spectrum at lower toroidal mode number compared to the other cases (Fig. 3, blue trace) [7]. Work is in progress to produce s-α diagrams to investigate the stability of these equilibria as the global beta is increased.

5. Core transport analysis - As the input power/total beta is increased, the DIII-D hybrid discharges described here exhibit improved confinement at otherwise similar pedestal pressure, especially at high δ. Thus, the higher plasma shaping allows for higher total pressure through improved edge stability, but the observed confinement improvement with beta is a core effect. Conversely, in AUG improved H-modes the observed confinement improvement at high beta with respect to the IPB98(y,2) scaling is due to improved pedestal confinement. It is thus interesting to investigate also the core transport in the two tokamaks.

To this end, the AUG and DIII-D beta scans have been analyzed performing gyrokinetic simulations with GYRO [8] to identify the dominant unstable modes and the proximity of the experiment to the linear threshold. Fig. 4 shows the dependence of the linear growth rate of the most unstable mode as a function of R/L_{Ti} at mid-radius ($\rho_{tor} = 0.5$) for the DIII-D low and high beta discharges at high δ. The most unstable mode is found to be an ion temperature gradient (ITG) mode, both at low and high β_N, and a significant stabilizing effect is due to the inclusion of electromagnetic effects (β_e) in the gyrokinetic model. A similar analysis for the low and high β_N phases of an AUG improved H-mode power scan confirms the non-negligible stabilizing effect of β_e on the ITG modes of these plasmas. The experimental point, in terms of the relevant parameter β_e, is much closer to the onset of kinetic ballooning modes in AUG than in DIII-D. This might explain why $R/L_{Ti}(\rho_{tor} = 0.5)$ increases from 5 ($\beta_N = 2.0$) to 5.7 ($\beta_N = 2.9$) in DIII-D, while it remains constant at ~ 6.1 as the input power is increased in the AUG scan (β_N from 1.9 to 2.7). This difference between the two machines is found despite a comparable increase by a factor of 2 in the (stabilizing) ExB shearing rate (calculated as in [9]) with β_N both in DIII-D and AUG.

6. Summary - Plasma shape is a useful tool to enhance hybrid performance through pedestal effects: higher δ leads to higher pedestal pressure and hence higher confinement factor at a given global beta, thus reducing the input power requirement to achieve the given beta. Non-stiffness of the core profiles, as displayed in the DIII-D discharges at high δ, leads to improved core confinement as the total beta is increased, while the pedestal pressure remains constant. In AUG improved H-modes the increase in global confinement is driven by the increase of the pedestal confinement for stiff plasma profiles.

Work supported in part by the US Department of Energy under DE-FC02-04ER54698.

References:

[1] C.F. Maggi et al., Nucl. Fusion 47 (2007) 535.
[2] A.C.C. Sips, this conference.
[3] P.A. Politzer et al., Nucl. Fusion 48 (2008) 075001.
[4] J. Stober et al., Nucl. Fusion 47 (2007) 728.
[5] A. Leonard et al., Phys. Plasmas 15 (2008) 056114.
[6] H. Urano et al., Nucl. Fusion 48 (2008) 045008.
[7] C. Konz et al., this conference, P2.071.
[8] J. Candy and R.E. Waltz, J. Comput. Phys. 186, 545 (2003).
[9] R.E. Waltz et al., Phys. Plasmas 4 (1997) 2482.

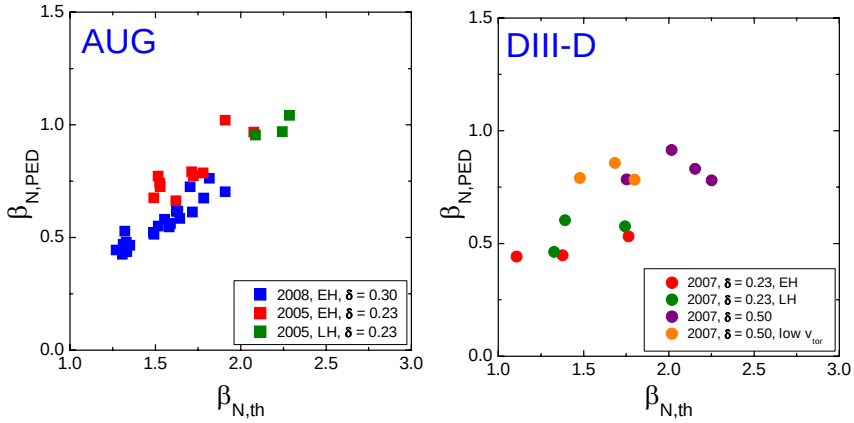

Figure 1. Pedestal vs total thermal beta for the AUG and DIII-D power scans.

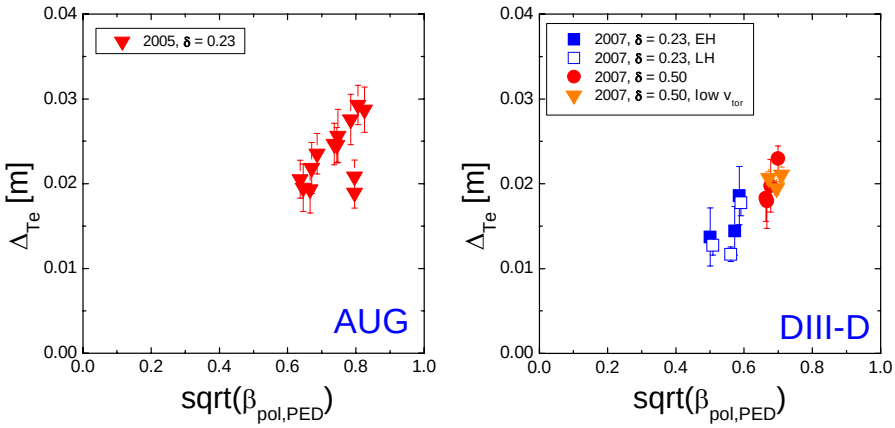

Figure 2. Te pedestal widths for AUG and DIII-D power scans vs sqrt($\beta_{pol,PED}$). The variation in β_{pol} is due to the variation in plasma shape in the DIII-D experiments and to the increase in input power in the AUG experiments.

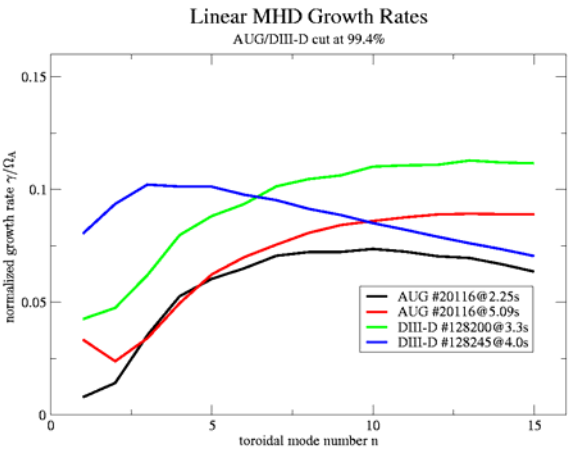

Figure 3. Growth rates normalized to the Alfven frequency vs the toroidal mode number for AUG and DIII-D: AUG, β_N = 1.9 (black); AUG, β_N = 2.7 (red); DIII-D, δ = 0.23 and β_N = 2.5 (green); DIII-D, δ = 0.5 and β_N = 2.7 (blue).

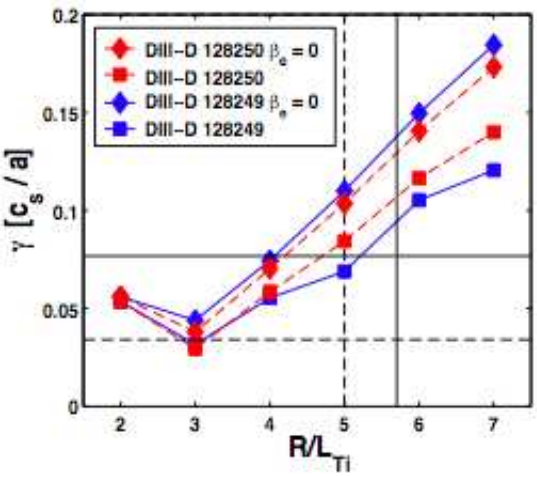

Figure 4. Growth rate of the most unstable mode at ρ_{tor}=0.5 vs R/L_{Ti} for the DIII-D case at β_N=2.0 (red, dashed lines) and at β_N=2.9 (blue, solid lines). Vertical lines identify the experimental values of R/L_{Ti} and horizontal lines the corresponding ExB shearing rate.